



Monitoring of carbon dioxide fluxes in a subalpine grassland ecosystem of the Italian Alps using a multispectral sensor

K. Sakowska^{1,2}, L. Vescovo¹, B. Marcolla¹, R. Juszczak², J. Olejnik^{2,3}, and D. Gianelle^{1,4}

¹Sustainable Agro-Ecosystems and Bioresources Department, Research and Innovation Centre – Fondazione Edmund Mach, Via E. Mach 1, 38010 – S. Michele all’Adige (TN), Italy

²Meteorology Department – Poznan University of Life Sciences, Piatkowska Street 94, 60-649 Poznan, Poland

³Department of Matter and Energy Fluxes, Global Change Research Center, AS CR, v.v.i. Belidla 986/4a, 603 00 Brno, Czech Republic

⁴Foxlab Joint CNR-FEM Initiative, Via E. Mach 1, 38010 – S. Michele all’Adige (TN), Italy

Correspondence to: K. Sakowska (karolina.sakowska@fmach.it)

Received: 3 February 2014 – Published in Biogeosciences Discuss.: 25 March 2014

Revised: 16 July 2014 – Accepted: 30 July 2014 – Published: 8 September 2014

Abstract. The study investigates the potential of a commercially available proximal sensing system – based on a 16-band multispectral sensor – for monitoring mean midday gross ecosystem production (GEP_m) in a subalpine grassland of the Italian Alps equipped with an eddy covariance flux tower. Reflectance observations were collected for 5 consecutive years, characterized by different climatic conditions, together with turbulent carbon dioxide fluxes and their meteorological drivers. Different models based on linear regression (vegetation indices approach) and on multiple regression (reflectance approach) were tested to estimate GEP_m from optical data. The overall performance of this relatively low-cost system was positive. Chlorophyll-related indices including the red-edge part of the spectrum in their formulation (red-edge normalized difference vegetation index, $NDVI_{red-edge}$; chlorophyll index, $CI_{red-edge}$) were the best predictors of GEP_m , explaining most of its variability during the observation period. The use of the reflectance approach did not lead to considerably improved results in estimating GEP_m : the adjusted R^2 ($adjR^2$) of the model based on linear regression – including all the 5 years – was 0.74, while the $adjR^2$ for the multiple regression model was 0.79. Incorporating mean midday photosynthetically active radiation (PAR_m) into the model resulted in a general decrease in the accuracy of estimates, highlighting the complexity of the GEP_m response to incident radiation. In fact, significantly higher photosynthesis rates were observed under diffuse as regards direct radiation conditions. The models which were observed to perform

best were then used to test the potential of optical data for GEP_m gap filling. Artificial gaps of three different lengths (1, 3 and 5 observation days) were introduced in the GEP_m time series. The values of $adjR^2$ for the three gap-filling scenarios showed that the accuracy of the gap filling slightly decreased with gap length. However, on average, the GEP_m gaps were filled with an accuracy of 73 % with the model fed with $NDVI_{red-edge}$, and of 76 % with the model using reflectance at 681, 720 and 781 nm and PAR_m data.

1 Introduction

In recent years, quantifying and understanding the dynamics and the main drivers of ecosystem carbon dioxide exchange, as well as upscaling the level of observations, have become critical challenges for the environmental scientific community (Canadell et al., 2000; Gamon et al., 2006; Running et al., 1999; Wohlfahrt et al., 2010).

The eddy covariance (EC) technique is a widely and commonly applied method to estimate carbon dioxide exchange between vegetation and the atmosphere at the ecosystem scale (Baldocchi, 2003; Burba, 2013; Geider et al., 2001). Although this method is able to provide direct, near-continuous and high-temporal resolution measurements of net gas exchange, it also has some limitations.

EC technique provides flux measurements of a relatively small area. The flux “footprint” varies from tens of meters to

several kilometers and depends on many parameters such as measurement height, wind velocity, surface roughness and atmospheric stability (Baldocchi, 2003; Kljun et al., 2001; Schmid, 1994). At the same time, the EC systems are relatively expensive – the typical cost for a complete EC system is on the order of USD 40–50 thousand, and the cost of site infrastructure is additional (Running et al., 1999). Considering all of these aspects, it is clear that, although EC measurements can be considered a solid basis for the ecosystem-scale CO₂ flux measurements, complementary methods are needed to extend the estimates to landscape and regional scales.

Important networks such as SpecNet, IMECC, and EU-ROSPEC have been investigating the potential of coupling spectral and EC observations (Balzarolo et al., 2011). In situ measurements can provide unique data sets with high spectral, spatial and temporal resolution, which represent a solid basis for validation of remote observations carried out at aircraft and satellite levels and further upscaling (Gamon et al., 2006; Gamon et al., 2010). As a result the number of sites where direct flux measurements are conducted simultaneously with in situ spectral measurements has increased significantly within the last decade.

The most commonly used approach to estimate the gross ecosystem production (GEP; $\mu\text{mol m}^{-2} \text{s}^{-1}$) with proximal sensing is based on the light-use efficiency (LUE) model proposed by Monteith (Monteith and Moss, 1977; Monteith, 1972). This simple model assumes that GEP is driven by the absorbed photosynthetically active radiation (APAR; $\mu\text{mol m}^{-2} \text{s}^{-1}$) and the photosynthetic radiation use efficiency expressing the carbon sequestration efficiency per amount of the absorbed solar energy (ε ; $\mu\text{mol CO}_2 \mu\text{mol}^{-1}$ APAR):

$$\text{GEP} = \varepsilon \cdot \text{APAR} = \varepsilon \cdot f_{\text{APAR}} \cdot \text{PAR}, \quad (1)$$

where PAR is the incident photosynthetically active radiation ($\mu\text{mol m}^{-2} \text{s}^{-1}$) and f_{APAR} is the fraction of PAR absorbed by the vegetation canopy (%).

Numerous studies have highlighted that spectral vegetation indices (VIs) are a non-direct measure of canopy “greenness”, which is a complex parameter comprising a whole range of vegetation properties such as f_{APAR} (Inoue et al., 2008; Myneni and Williams, 1994; Sims et al., 2006; Walter-Shea et al., 1997), leaf area index – LAI (Gitelson et al., 2003c; Rossini et al., 2012; Serrano et al., 2000; Stenberg et al., 2004; Vescovo and Gianelle, 2008; Viña et al., 2011), chlorophyll content (Gitelson et al., 2005; Rossini et al., 2012; Wu et al., 2008), green herbage ratio (Gianelle and Vescovo, 2007; Vescovo and Gianelle, 2006) and fractional vegetation cover (Carlson and Ripley, 1997; Glenn et al., 2008).

In non-stressed ecosystems characterized by strong seasonal dynamics such as some managed croplands, independent estimates of ε may be unnecessary due to its relation with the chlorophyll content (Gitelson et al., 2012; Peng and Gitelson, 2012; Peng et al., 2011; Rossini et al., 2012; Wu

et al., 2009), and this is particularly true when integrating GEP over longer timescales, e.g., days (Gitelson et al., 2008). Therefore most of the variations in plant productivity in such ecosystems should be reflected by changes in APAR (Lobell et al., 2002).

Several studies modeled GEP as a function of VIs (Harris and Dash, 2010; Rossini et al., 2010; Sims et al., 2006; Sjöström et al., 2009; Xiao et al., 2004) and/or of VIs multiplied by PAR (Gitelson et al., 2006; Peng and Gitelson, 2012; Peng et al., 2011). Including PAR in the model should theoretically enhance the correlation with GEP, because the product of VI and PAR takes into account the seasonal changes in both biophysical parameters controlling the photosynthesis process (e.g., f_{APAR} and chlorophyll content) and in the amount of radiation reaching the vegetation surface (Gitelson et al., 2012).

In the current study, 5 years of field multispectral data acquired with the CROPSCAN MSR16R system (CROPSCAN Inc., Rochester, USA) deployed on the EC tower of the FLUXNET grassland site IT-MBo (Viote del Monte Bondone, Trento, Italy) are presented and analyzed.

In particular, the objectives of this paper are the following:

- (i) to investigate the potential of vegetation reflectance and narrow-band VIs for monitoring carbon dioxide fluxes exchanged between the dynamic grassland ecosystem and the atmosphere
- (ii) to analyze the relationships between spectral data and carbon dioxide fluxes during the 5 years of observations in order to determine how robust the relationships between vegetation spectral properties (reflectance and narrow-band VIs) and mean midday GEP (GEP_m) are
- (iii) to compare different approaches (correlation analysis and multiple regression) to estimate GEP_m
- (iv) to evaluate the potential of spectral models to gap-fill GEP_m data.

2 Materials and methods

2.1 Experimental site

The study site is a permanent alpine grassland located at 1550 m a.s.l. on the Viote del Monte Bondone plateau (46°00' N, 11°02' E; Italian Alps).

The vegetation of the area is dominated by *Festuca rubra* (L.) (covering 25 % of the area), *Nardus stricta* (L.) (13 %) and *Trifolium* sp. (L.) (14.5 %), and is representative of a typical low-productive meadow of the Alps. The site is managed as an extensive meadow with low-mineral fertilization (applied in autumn) and is cut once a year, usually in mid-July (Gianelle et al., 2009). The maximum canopy height at the peak of the growing season (mid-June to early July) can reach approximately 30 cm.

The climate of this area is sub-continental (warm and wet summer) and is characterized by a mean annual temperature of 5.5 °C, with monthly averages ranging from −3.1 °C in February to 14.3 °C in July. The annual mean precipitation is 1244 mm, with maximum values in May (138 mm) and October (162 mm). The snow-free period lasts typically from early May to late October (Marcolla et al., 2011).

The site is characterized by a regular east–west wind circulation, showing along this direction an almost flat topography with a homogeneous vegetated fetch of more than 500 m. An experimental footprint analysis demonstrated that 30 % (in stable atmospheric conditions) to 80 % (in unstable conditions) of the total CO₂ flux originates within 30 m from the EC tower (Marcolla and Cescatti, 2005).

2.2 Eddy covariance and meteorological data

Continuous EC measurements of CO₂, water vapor and sensible heat fluxes were performed at the Monte Bondone FLUXNET site from the beginning of August 2002. In the present study, data from 2008 to 2012 were used, to match the available spectral data set.

The eddy covariance (EC) system consisted of a Licor Li-7500 open-path infrared gas analyzer (Li-COR Inc., Lincoln, Nebraska, USA) and a Gill R3 3-D ultrasonic anemometer (Gill Instruments Ltd., Lymington, UK), mounted at a height of 2.5 m. Raw data were recorded at a frequency of 20 Hz and stored by means of the EDISOL software package (Moncrieff et al., 1997). The EdiRE software (version 1.4.3.1021, R. Clement, University of Edinburgh) was used to compute turbulent CO₂ fluxes from the raw data.

Along with EC flux measurements, the main meteorological and soil physical variables were measured, including the following: short- and long-wave radiation components (Kipp & Zonen CNR1, Delft, the Netherlands), incoming total and diffuse PAR (LI-COR LI-190SA, Lincoln, USA; and Delta-T BF3H, Cambridge, UK), precipitation (Young 52202H, Traverse City, Michigan, USA), air humidity and temperature (Rotronic MP103A, Crawley, UK), soil temperature profile at depths of 2, 5, 10, 20 and 50 cm (STP01, Hukseflux, Delft, the Netherlands), and volumetric soil water content at depths of 10 and 20 cm (CS615 reflectometers, Campbell Scientific Inc., Logan, Utah, USA). All meteorological variables were recorded at 1 min intervals and averaged over 30 min; both 1 min data and half-hourly averages were stored on a CR23X data logger (Campbell Scientific Inc., Logan, Utah, USA).

Half-hourly measurements of net ecosystem exchange (NEE) were gap-filled and partitioned into ecosystem respiration (Reco) and gross ecosystem production (GEP) by means of the online tool developed by Reichstein et al. (2005) (<http://www.bgcjena.mpg.de/bgcmdi/html/eddyproc>). However, only non-gap-filled data were analyzed in this study.

Table 1. Multispectral CROPSCAN MSR16R system specifications.

CROPSCAN multispectral radiometer (MSR16R)			
Band number	Channel name	Center wavelength (nm)	Bandwidth (nm)
1	R470	469.0	8.8
2	R531	531.1	8.0
3	R547	546.7	8.7
4	R570	569.6	10.4
5	R610	610.1	9.3
6	R640	639.8	10.0
7	R681	681.4	10.7
8	R720	720.2	9.6
9	R730	730.4	10.2
10	R750	749.5	10.6
11	R781	781.0	9.8
12	R861	861.4	10.5
13	R902	901.6	8.7
14	R979	979.1	10.2
15	R1238	1238.0	10.6
16	R1660	1659.8	14.4

To maintain consistency between the time window used for calculating vegetation reflectance and narrow-band VIs, the mean midday gross ecosystem production (GEP_m, μmol m^{−2} s^{−1}) and mean midday incoming photosynthetically active radiation (PAR_m, μmol m^{−2} s^{−1}) were calculated for the same time period used for vegetation spectral properties (11:00 a.m.–1:00 p.m. of local solar time).

Further details regarding the EC instrumentation, data elaboration and quality control can be found in Marcolla et al. (2011).

2.3 Multispectral reflectance and narrow-band vegetation indices

Multispectral data were acquired on a continuous basis from 2008 to 2012 by means of the CROPSCAN multispectral radiometer system MSR16R (CROPSCAN Inc., Rochester, USA). The system consists of a 16-band radiometer (simultaneously measuring reflected and incoming radiation in narrow spectral bands) and a data logger controller (DLC) storing the acquired data (Table 1). For each band, the incoming solar irradiance is measured through a cosine diffuser, while reflected radiance is measured through a 28° field of view foreoptic. The system was installed on the existing EC tower at a height of 6 m, which allowed the observation of a 3.0 m diameter vegetation surface. The instrument was operated during five growing seasons (15 May–21 November 2008, 20 May–1 November 2009, 19 May–24 October 2010, 11 May–3 September 2011 and 18 May–30 September 2012), for a total of 758 days.

Before the beginning of each growing season, the system was calibrated using the method recommended by the manufacturer, based on the use of a white reference panel with known reflectance (<http://www.cropscan.com/wsuptdn.html>). Additionally, CROPSCAN, Inc. provided cosine response calibration data with each upward-facing MSR16 module and temperature sensitivity calibration data. Both cosine and temperature corrections were included in the postprocessing software (POSTPROC program) provided with the MSR system.

Incident irradiance and reflected radiance were collected every 10 min, and reflectance at given wavelengths was calculated. In order to minimize solar angle effects, reflectance data were finally averaged over 2 h close to a solar noon (11:00 a.m.–1:00 p.m. of local solar time).

Due to the noisy and unreliable optical signal beyond 1000 nm (bands no. 15 and 16; Table 1), only the data of the first 14 bands were included in the analyses. In addition, data were excluded when (1) the site was covered by snow, (2) precipitation was recorded 2 h prior or during the mid-day averaging period, and (3) the weather conditions did not allow for the removal of the cut biomass from the footprint of CROPSCAN system (and EC tower) straight after the cut event. According to these quality criteria, 24 % of the data were discarded, mainly due to the meteorological conditions.

Canopy reflectance spectra were then used for computing the VIs. Although many different VIs were investigated (Table A1), only the most commonly used and the best performing in GEP_m estimation – considering all the 5 years of observations – are presented in the study. The list of the five presented VIs is reported in Table 2.

2.4 Models for GEP_m estimation

In order to estimate GEP_m we used two approaches: one based on linear regression (using the concept of the LUE model, i.e., Eq. 1) and the other on multiple regression. The first approach assumed a direct linear relationship between GEP_m and VIs (model 1) and between GEP_m and the product of VIs and PAR_m (model 2). In the second approach, the interaction effects between different variables were explored by running two stepwise bidirectional multiple regression models, in which GEP_m was set as a dependent variable and reflectance (model 3), or reflectance and PAR_m (model 4), as explanatory variables. The abovementioned models (Table 3) were tested both for each year on a separate basis, and for all the years together in order to obtain the general models for the estimation of GEP_m.

2.5 Statistical analysis

Pearson's correlation analysis was used to test the significance of the relationships between GEP_m and VIs · PAR_m.

In order to evaluate how robust the relationships between GEP_m and VIs were, the slopes of the linear regressions be-

tween the best performing VI against GEP_m were analyzed. In particular, the slopes of the regressions obtained for each year and obtained in the general model 1 (including all 5 years) were compared by means of a *t* test to check whether the regression coefficients were statistically different.

Besides, a multiple stepwise bidirectional linear regression was used to explore the interaction effects between variables (considering GEP_m as a dependent variable and reflectance at 14 analyzed wavelengths (model 3), or reflectance values and PAR_m (model 4), as explanatory variables) to find the model that best fits the data according to Akaike's information criterion (AIC; Akaike, 1973). The variance inflation factor (VIF; Mason et al., 2003) was used to measure the degree of (multi)collinearity of the *i*th independent variable with the other independent variables in the regression models.

When VIF for any of the predictors reached the threshold value of 10, the (multi)collinearity was reduced by eliminating one independent variable (the last one selected by the automatic stepwise bidirectional regression) from the analysis (O'Brien, 2007). The procedure was repeated until none of the VIF factors exceeded the acceptable threshold value; thus the subset of explanatory variables was free of significant (multi)collinearity issues.

The final subset of the predictor variables was selected by testing whether the increase of the adjusted R^2 ($adjR^2$) after adding a subsequent predictor variable to the multiple regression model was significantly different from zero (at significance level $\alpha = 0.001$). Multiple regression models were compared by means of the Fisher test.

Each of the four model's coefficients was obtained by fitting each model against GEP_m. The main goodness of fit statistics (adjusted coefficient of determination – $adjR^2$, root mean square error – RMSE, percentage root mean square error – PRMSE and probability value – *p*) were computed to compare the performance of the different models.

Additionally, a validation of the best performing general models using training/validation splitting approach, in which 1 year at a time was excluded from the data set, was conducted. The remaining 4-year subset was used as a training set and the excluded year as a validation set. The model was fitted (calibrated) against each training set and the resulting parameterization was used to predict the GEP_m of the excluded year. Validation accuracy was evaluated in terms of RMSE.

All the statistical analyses were performed by means of the R software (version 2.15.2, <http://www.r-project.org>).

2.6 The gap scenarios

In order to evaluate the ability of spectral models to gap-fill CO₂ flux data, secondary data sets were generated by flagging ~16 % of the five growing seasons data as unavailable (artificial gaps constituting 90 observation days out of 573 available observation days). The percentage of artificial gaps

Table 2. Spectral vegetation indices presented in this study: normalized difference vegetation index (NDVI), modified simple ratio (MSR), difference ratio (DR), red-edge normalized difference vegetation index (NDVI_{red-edge}), and chlorophyll index (CI_{red-edge}). R refers to reflectance at a specific band (nm).

Index	Formulation	Reference
NDVI	$(R750 - R681)/(R750 + R681)$	Rouse et al. (1973)
MSR	$(R750/R681 - 1)/(R750/R681 + 1)^{1/2}$	Haboudane et al. (2004)
DR	$(R750 - R720)/(R750 - R681)$	Datt (1999)
NDVI _{red-edge}	$(R750 - R720)/(R750 + R720)$	Gitelson and Merzlyak (1994)
CI _{red-edge}	$(R750/R720) - 1$	Gitelson et al. (2003a)

Table 3. The four models for GEP_m estimation tested in the presented study.

Model	Model formulation
1	$GEP_m = b_0 + b_1 VI$
2	$GEP_m = b_0 + b_1 (VI \cdot PAR_m)$
3	$GEP_m = b_0 + b_1 R470 + b_2 R531 + b_3 R547 + b_4 R570 + b_5 R610 + b_6 R640 + b_7 R681 + b_8 R720 + b_9 R730 + b_{10} R750 + b_{11} R781 + b_{12} R861 + b_{13} R902 + b_{14} R979$
4	$GEP_m = b_0 + b_1 R470 + b_2 R531 + b_3 R547 + b_4 R570 + b_5 R610 + b_6 R640 + b_7 R681 + b_8 R720 + b_9 R730 + b_{10} R750 + b_{11} R781 + b_{12} R861 + b_{13} R902 + b_{14} R979 + b_{15} PAR_m$

was chosen due to the fact that during the observation period of the study (~May to November, 2008–2012) the EC data set had an average of 16% of missing or rejected values of NEE data collected during midday hours. Following Moffat et al. (2007) these artificial gaps were superimposed on the already incomplete data, without regard for the distribution of real gaps in the time series. Three gap length scenarios were considered: gaps of 1, 3 and 5 observation days. The artificial gaps were distributed randomly, and each of the three scenarios was permuted 10 times and results were averaged (Moffat et al., 2007). Secondary data sets with artificial gaps were used to calibrate the models that were applied for filling GEP_m data. The gap-filling statistical metrics (adjR², RMSE, PRMSE) were calculated using the EC derived GEP_m in these artificial gaps to validate the predictions of filling technique.

3 Results

Figure 1 shows the seasonal variations of (a) PAR_m and (b) GEP_m. During the snow-free period (May–November) the average PAR_m was 1073 (±472), 1167 (±485), 1068 (±581), 1199 (±463) and 1065 (±523) μmol m⁻² s⁻¹ in 2008, 2009, 2010, 2011 and 2012, respectively, with maximum values of approximately 2000 μmol m⁻² s⁻¹. The maximum difference in PAR_m means among the investigated growing seasons was less than 11.5%. Mean daily air temperature (Fig. 2) for the same period was 9.1 (±5.3), 10.0 (±5.2), 8.4 (±5.6), 9.8 (±4.8) and 10.0 (±5.3) °C in 2008, 2009, 2010, 2011 and 2012, respectively, and the maximum difference between temperature means was equal to 15.6%. A higher

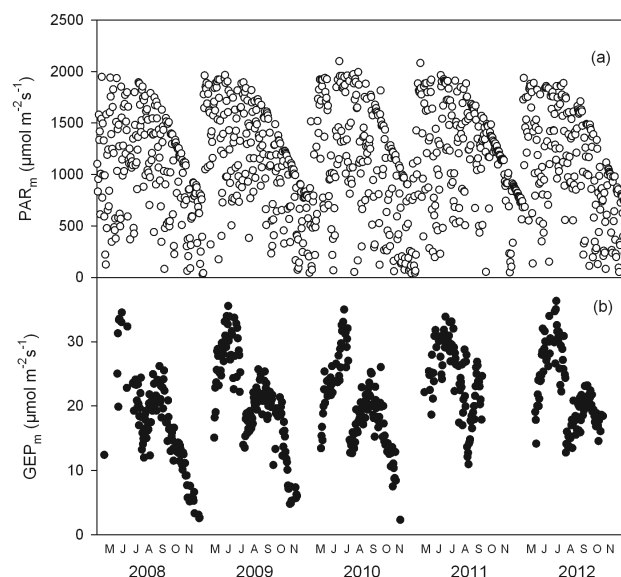


Figure 1. Seasonal variation of (a) mean midday PAR (PAR_m; μmol m⁻² s⁻¹) and (b) mean midday GEP (GEP_m; μmol m⁻² s⁻¹) in the growing seasons of 2008–2012.

variability was observed in total precipitation recorded from May to November (Fig. 2). The differences in precipitation sums between the investigated years reached up to 50%. The precipitation amount in 2011 (1008 mm) was similar to the 20-year period average (990 mm, 1993–2012). The growing season of 2010 (1473 mm) was particularly wet, with a precipitation sum 49% higher than the long term average, while 2009 (744 mm) was fairly dry, with a total precipitation

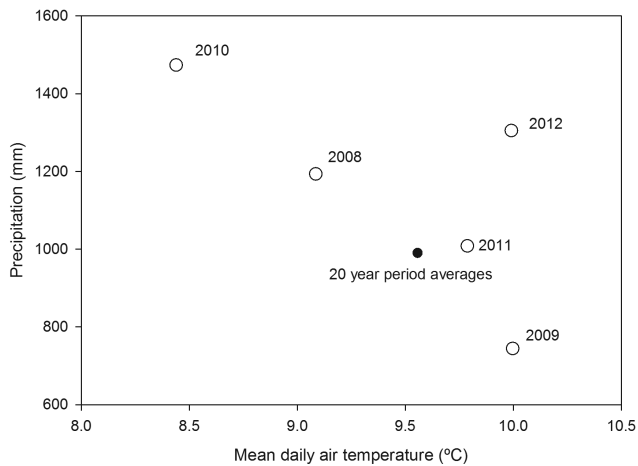


Figure 2. Cumulative precipitation versus average daily air temperature for the period May–November.

25 % lower than the average sum of precipitation in 1993–2012. The precipitation amounts in 2008 (1193 mm) and 2012 (1305 mm) were higher than the 20-year period average by 21 % and 32 %, respectively.

Seasonal patterns of GEP_m were driven by both environmental variables (such as incoming PAR and air temperature) and grassland management (Marcolla et al., 2011). The grassland cut occurred around mid-July, and split the growing season into two sub-periods. The maximum gross CO₂ flux rates were recorded in the early summer (end of June – mid July). After the cut event, the canopy regrowth generally reached a peak at the beginning of September.

The VIs showed a similar behavior to GEP_m, and the peaks of these time series were almost synchronous. Starting from the early part of September, VIs began decreasing gradually in all the investigated years due to the senescence phase (characterized by a progressive canopy yellowing and wilting), but at varied rates.

Examples of seasonal courses of investigated VIs and GEP_m measured in 2012 are shown in Fig. 3. For better visualization and easier comparison, both GEP_m and VIs were normalized by scaling between 0 and 1. The graphs which refer to other years of observations can be found in Appendix Fig. B1.

The linear regression analysis (Table 4) showed that the presented VIs explained at least 50 % of the variability of GEP_m.

The highest accuracy of model 1 was obtained in 2009 and 2012 ($adjR^2$ up to 0.81). On the other hand, the lowest accuracy of the same model was reported in 2011 (max $adjR^2 = 0.64$). This low value of $adjR^2$ could be explained by the fact that during this year the CROPSCAN sensor was not operated during the autumn period, and thus the range of VIs and GEP_m was smaller as the senescence phase was missed (Table 4).

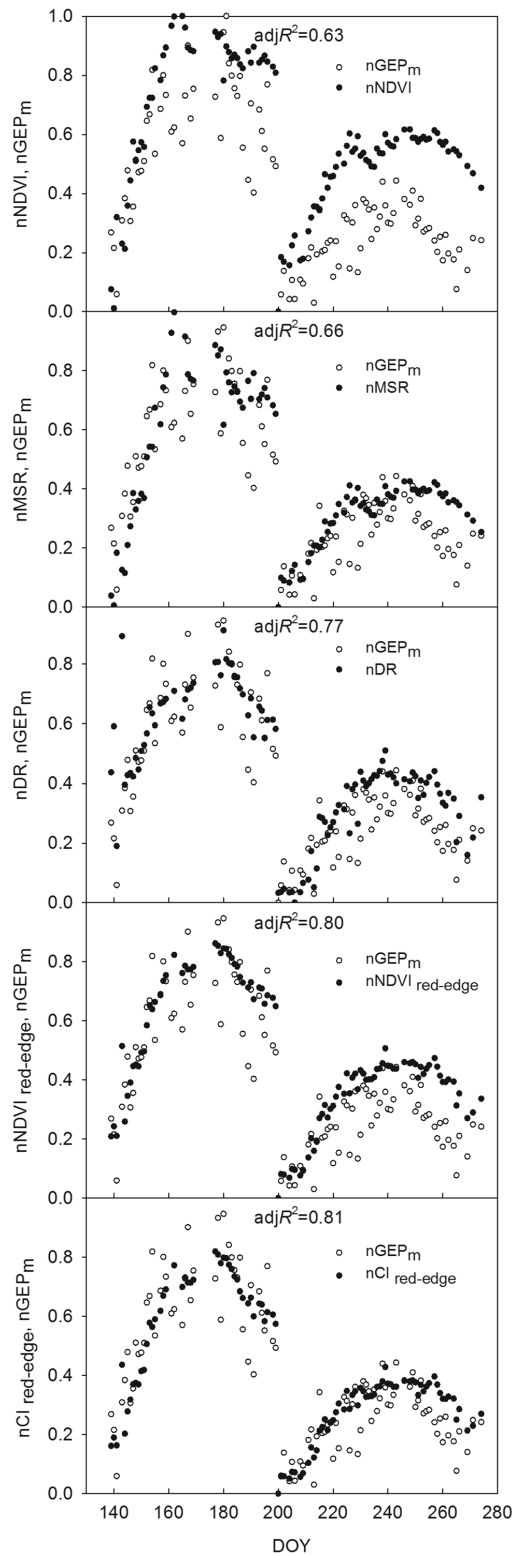


Figure 3. Seasonal courses of normalized spectral vegetation indices – nVIs (–) and normalized mean midday gross ecosystem production – nGEP_m (–) in the growing season of 2012; $adjR^2$ between GEP_m estimated from EC measurements and GEP_m obtained with model 1 fed with the various VIs.

Table 4. Summary of the statistics (n – number of observations, $\text{adj}R^2$ – adjusted coefficient of determination, RMSE – root mean square error, PRMSE – percentage root mean square error) of the two linear regression models tested in this study both annually and considering all of the 5 observation years together. The three best-fitting models in each group are printed in bold. The best performing model is additionally highlighted in italic. All the regressions were statistically significant ($p < 0.01$).

Model	VIs	Meteo	2008				2009				2010			
			data		RMSE	PRMSE	data		RMSE	PRMSE	data		RMSE	PRMSE
			n	$\text{adj}R^2$			n	$\text{adj}R^2$			n	$\text{adj}R^2$		
–	–	$\mu\text{mol m}^{-2} \text{s}^{-1}$	%	–	–	$\mu\text{mol m}^{-2} \text{s}^{-1}$	%	–	–	$\mu\text{mol m}^{-2} \text{s}^{-1}$	%			
1	NDVI	–	0.65	3.97	22.95	0.80	3.12	14.88	–	0.64	3.71	18.50		
	MSR	–	0.70	3.66	21.16	0.81	3.09	14.72	–	0.68	3.53	17.59		
	DR	–	0.60	4.23	24.43	0.74	3.59	17.12	123	0.64	3.72	18.55		
	NDVI _{red-edge}	–	0.70	3.66	21.14	0.81	3.04	14.49	–	0.69	3.45	17.20		
	CI _{red-edge}	–	0.71	3.59	20.76	0.76	3.48	16.58	–	0.68	3.50	17.47		
2	NDVI	PAR _m	0.55	4.49	25.96	0.41	5.40	25.76	–	0.40	4.81	23.98		
	MSR	PAR _m	0.62	4.14	23.94	0.53	4.84	23.07	–	0.64	3.73	18.59		
	DR	PAR _m	0.50	4.75	27.47	0.40	5.47	26.07	123	0.38	4.88	24.33		
	NDVI _{red-edge}	PAR _m	0.65	3.96	22.89	0.56	4.69	22.36	–	0.60	3.92	19.52		
	CI _{red-edge}	PAR _m	0.68	3.79	21.89	0.60	4.46	21.30	–	0.70	3.38	16.83		
Model	VIs	Meteo	2011				2012				2008–2012			
			data		RMSE	PRMSE	data		RMSE	PRMSE	data		RMSE	PRMSE
			n	$\text{adj}R^2$			n	$\text{adj}R^2$			n	$\text{adj}R^2$		
–	–	$\mu\text{mol m}^{-2} \text{s}^{-1}$	%	–	–	$\mu\text{mol m}^{-2} \text{s}^{-1}$	%	–	–	$\mu\text{mol m}^{-2} \text{s}^{-1}$	%			
1	NDVI	–	0.53	3.70	15.16	0.63	3.40	15.36	–	0.63	4.07	19.57		
	MSR	–	0.50	3.80	15.57	0.66	3.24	14.65	–	0.64	4.04	19.43		
	DR	–	0.64	3.22	13.20	0.77	2.66	12.05	573	0.67	3.87	18.64		
	NDVI _{red-edge}	–	0.61	3.37	13.80	0.80	2.50	11.29	–	0.74	3.41	16.40		
	CI _{red-edge}	–	0.61	3.36	13.74	0.81	2.46	11.10	–	0.73	3.47	16.72		
2	NDVI	PAR _m	0.55	3.60	14.73	0.28	4.75	21.49	–	0.47	4.90	23.58		
	MSR	PAR _m	0.66	3.14	12.86	0.59	3.60	16.29	–	0.60	4.24	20.43		
	DR	PAR _m	0.32	4.42	18.09	0.18	5.07	22.91	573	0.41	5.13	24.71		
	NDVI _{red-edge}	PAR _m	0.61	3.38	13.82	0.42	4.25	19.21	–	0.61	4.19	20.18		
	CI _{red-edge}	PAR _m	0.66	3.12	12.79	0.57	3.67	16.60	–	0.67	3.87	18.65		

The estimation accuracy was also dependent on the VIs used for the parameterization of model 1 (Table 4). VIs, including the red-edge band in their formulation, turned out to be the best candidates for GEP_m estimations considering both the general model and the 5 different years on a separate basis. The MSR, although it is based on the NIR and red bands, also showed reliable performance. Taking into account the models for the single years, MSR, DR, and CI_{red-edge} were included in the group of the three best fitting models 3, 2 and 4 times, respectively. NDVI_{red-edge} was in the group of the three best performing models in each investigated year. On the contrary, NDVI was never included among the best predictors of GEP_m (Table 4).

The best estimation accuracy obtained when model 1 was parameterized with NDVI_{red-edge} resulted in PRMSE of 21.14 %, 14.49 %, 17.20 %, 13.80 % and 11.29 % for 2008, 2009, 2010, 2011 and 2012, respectively. The comparison of linear regression slopes between NDVI_{red-edge} against GEP_m between each single year and the general model (which considered all 5 years of observation together) (Fig. 4) showed that only the slopes of these linear relationships in 2011 and 2012 were significantly different from the general model ($p = 0.02$ and 0.01 for 2011 and 2012, respectively). The other years (2008, 2009, 2010) were statistically indistin-

guishable from the general model (slopes: $p > 0.90$, $p > 0.46$, $p > 0.89$ for 2008, 2009, 2010, respectively). This contributed to the fact that NDVI_{red-edge} explained more than 74 % of the variability of GEP_m during the 5 years of observations (PRMSE of 16.40 %) (Table 4).

The inclusion of incoming PAR_m into the model resulted in a general decrease of its performance. The PRMSE was on average 14.64 % higher in model 2 than in model 1 considering all of the 5 years of observations. As an example, the $\text{adj}R^2$ of the general model (2008–2012) fed with NDVI_{red-edge} decreased from 0.74 to 0.61, RMSE increased from 3.41 to 4.19 $\mu\text{mol m}^{-2} \text{s}^{-1}$ and PRMSE increased from 16.40 to 20.18 %. A similar pattern was observed in each of the investigated years (Table 4).

In order to investigate the impact of radiation quality on these results, the light response of half-hourly GEP (data collected between 11:00 a.m. and 1:00 p.m.; during the snow-free period of 2012) considering different levels of diffuse radiation was investigated. Two different relationships between GEP and incoming PAR were found: one for cloudy conditions (when diffusion index – DI, which is the ratio between diffuse and total incident PAR, exceeded 0.7) and one for sunny conditions ($\text{DI} < 0.3$) (Fig. 5). The data when the abovementioned populations were overlapping (PAR from

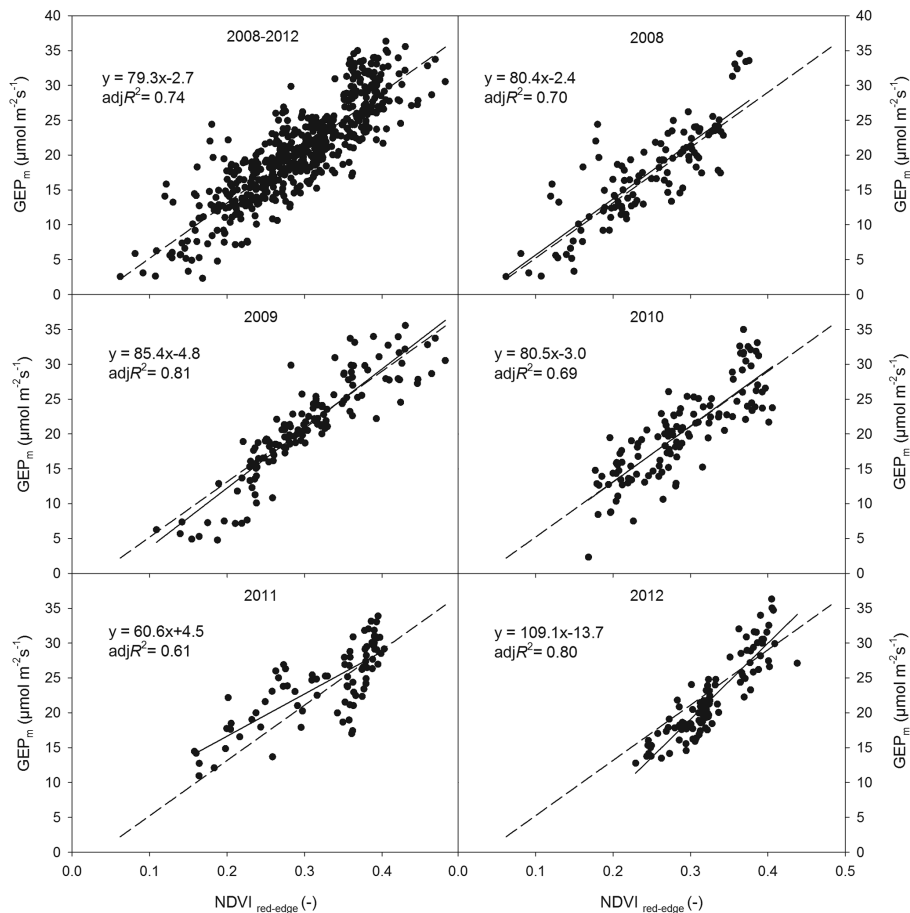


Figure 4. Relationship between the red-edge normalized difference vegetation index ($\text{NDVI}_{\text{red-edge}}$) and mean midday gross ecosystem production (GEP_m), considering both the 5 years of observation together and annual observations. Dashed and solid trend lines refer to the general model 1 (considering each year of observation) and model 1 based on the observations from a specific year, respectively.

800 to $1350 \mu\text{mol m}^{-2} \text{s}^{-1}$) indicated that, in the Monte Bondone grassland site, photosynthesis rates were significantly higher under diffuse compared to direct radiation.

A stepwise bidirectional procedure selected reflectance (R) at 681, 781 and 720 nm (model 3) and R681, R781, PAR_m and R720 (model 4) as significant drivers of GEP_m , considering each of the 5 years of observations simultaneously (Table 5).

It is interesting to note that in both model 3 and 4, referring to each observation year on a separate basis (data not shown), the red-edge bands were included as important predictors in all of the 5 investigated years. In model 3 the red region was chosen as a highly predictive variable in 40 % of cases, while the NIR region in three out of five investigated growing seasons. In model 4, red and NIR bands contributed to the stepwise regression model in 3 and 2 out of 5 observation years, respectively. PAR_m , as an additional variable of model 4, was included in the model three out of five times. The range of $\text{adj}R^2$ values for different years considered on a

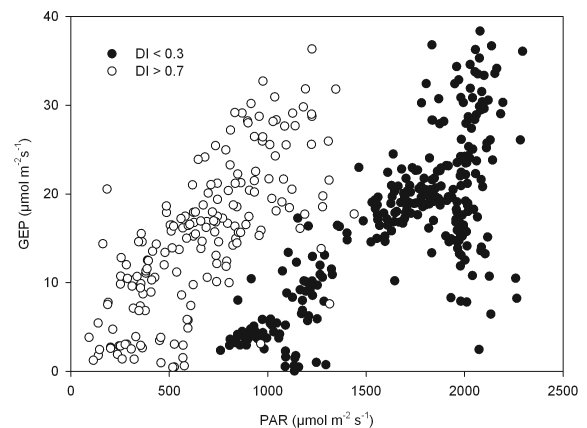


Figure 5. Light response of half-hourly gross ecosystem production (GEP ; from 11:00 a.m. to 1:00 p.m.) to the incident photosynthetically active radiation (PAR) in the snow-free period of 2012 (May–November). Diffusion index (DI) is the ratio between diffuse and total incident PAR . It ranges from 0 to 1.

Table 5. Summary of the general multiple regressions: partial adjusted R^2 , variance inflation factor (VIF), significance levels of the predictor variables (p), number of observations (n), cumulative adjusted R^2 , root mean square error (RMSE) and percentage root mean square error (PRMSE). R refers to reflectance at a given waveband (e.g., R720 – reflectance at 720 nm).

Model	Explanatory variables	Partial adjusted R^2	VIF	p	n	Cumulative adjusted R^2	RMSE	PRMSE
3	R681	0.44	5.65	0.00412	573	0.73	3.50	16.83
	R781	0.26	3.54	$< 2e-16$				
	R720	0.04	6.78	$< 2e-16$				
4	R681	0.44	5.69	0.0323	573	0.79	3.06	14.75
	R781	0.26	6.74	$< 2e-16$				
	PAR _m	0.07	1.25	$< 2e-16$				
	R720	0.03	7.25	$2.60e-16$				

separate basis varied from 0.61 to 0.87 and from 0.70 to 0.88 for model 3 and 4, respectively (data not shown).

A stepwise bidirectional multiple regression with reflectance at 681, 781 and 720 nm as predictors did not yield any improvement in the explained variance of GEP_m when the entire data set was considered ($\text{adj}R^2=0.74$ – general model 1; $\text{adj}R^2=0.73$ – general model 3; Table 4 and 5, respectively). Also, adding PAR_m as an independent variable of the model resulted only in a slight improvement in the accuracy of the GEP_m estimation compared to the general linear regression model 1 based on NDVI_{red-edge}. In fact, the $\text{adj}R^2$ increased from 0.74 to 0.79, while the PRMSE decreased from 16.40 to 14.75 % (Tables 4 and 5).

Validation of model 1 based on NDVI_{red-edge} showed that there was no relevant difference in prediction accuracy among validation years (RMSE was varying between 3.12 and 3.85 $\mu\text{mol m}^{-2} \text{s}^{-1}$, Fig. 6). Validation results of general model 4 showed that considering all the 5 validated years RMSE was on average 3.26 $\mu\text{mol m}^{-2} \text{s}^{-1}$.

The differences in the $\text{adj}R^2$ performance of the gap-filling scenarios showed that the accuracy of gap filling decreased slightly with gap length, while the range of the goodness of fit statistics ($\text{adj}R^2$, RMSE, PRMSE) generally increased with gap size (Table 6). However, on average, GEP_m gaps were filled with an accuracy of 73 % with model 1 fed with NDVI_{red-edge} (RMSE = 3.40 $\mu\text{mol m}^{-2} \text{s}^{-1}$, PRMSE = 16.48 %), and with an accuracy of 76 % (RMSE = 3.14 $\mu\text{mol m}^{-2} \text{s}^{-1}$, PRMSE = 15.25 %) with model 4 using reflectance at 681, 720 and 781 nm and PAR_m data.

4 Discussion

Continuous and simultaneous measurements of narrow-band canopy reflectance and EC carbon dioxide fluxes have been successfully performed for 5 consecutive years in a subalpine grassland ecosystem. The multispectral CROPSCAN MSR16R system demonstrated to be a reliable instrument for

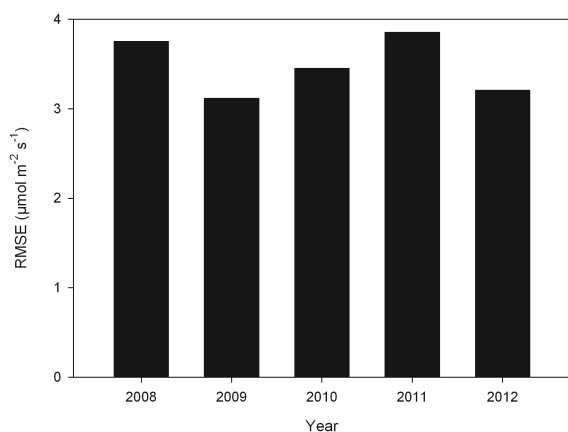
monitoring carbon dioxide fluxes. The results of this study provided important information on how consistent and robust the relationships between VIs and GEP_m are in such a dynamic ecosystem. Additionally, they allowed the comparison of different approaches (correlation analysis and multiple regression) for predicting GEP_m.

Although several studies have already compared VIs obtained from in situ observations against EC CO₂ fluxes (Gitelson et al., 2003b; Inoue et al., 2008; Peng and Gitelson, 2012; Peng et al., 2011; Rossini et al., 2010; Sims et al., 2006), and a few studies have focused on very similar canopies (Gianelle et al., 2009; Rossini et al., 2012; Wohlfahrt et al., 2010), we are not aware of any study based on such a long time series, acquired on a continuous basis during the growing seasons.

From the data presented, it follows that MSR and DR indices, which are modified and improved variants of the most commonly used VIs, showed generally a slightly stronger linear relationship with GEP_m when compared to NDVI. Nevertheless, considering all of the observation years, the most robust estimates of GEP_m were obtained when NDVI_{red-edge} and CI_{red-edge} were used to parameterize the model (Table 4). These results confirmed the findings of previous studies on both similar (Rossini et al., 2012) and different ecosystems (Gitelson et al., 2003b; Peng and Gitelson, 2012; Peng et al., 2011; Rossini et al., 2010), indicating that VIs based on the red-edge part of the spectrum are the most sensitive to the seasonal GEP dynamics due to their better linearity with chlorophyll content (Gitelson et al., 2003a; Sims and Gamon, 2002; Wu et al., 2008), and with green leaf area index – green LAI (Gitelson et al., 2003c; Viña et al., 2011). In general, VIs (such as NDVI) calculated as a normalized difference between NIR bands – characterized by a high reflectance due to leaf and canopy scattering, and visible bands (e.g., red), where absorption by the chlorophyll pigments is predominant (Jackson and Huete, 1991) – tend to lose their sensitivity to moderate–high aboveground biomass due to the saturation of reflectance in the visible bands and due to the limitation of the normalized difference approach

Table 6. Summary of the statistical metrics of gap-filling procedure: adjusted R^2 ($\text{adj}R^2$), root mean square error (RMSE) and percentage root mean square error (PRMSE).

Model	Input variables	Gap length									
		1 observation day			3 observation days			5 observation days			
		$\text{adj}R^2$ –	RMSE $\mu\text{mol m}^{-2} \text{s}^{-1}$	PRMSE %	$\text{adj}R^2$ –	RMSE $\mu\text{mol m}^{-2} \text{s}^{-1}$	PRMSE %	$\text{adj}R^2$ –	RMSE $\mu\text{mol m}^{-2} \text{s}^{-1}$	PRMSE %	
1	NDVI _{red-edge}	mean	0.76	3.41	16.45	0.72	3.43	16.71	0.70	3.34	16.28
		range	0.16	0.73	3.80	0.28	1.19	5.45	0.46	0.95	6.50
4	R681	mean	0.78	3.16	15.25	0.77	3.10	15.08	0.73	3.17	15.42
	R781		0.14	0.46	2.72	0.18	0.81	4.23	0.33	0.75	5.13
	PAR _m	range	0.14	0.46	2.72	0.18	0.81	4.23	0.33	0.75	5.13
	R720		0.14	0.46	2.72	0.18	0.81	4.23	0.33	0.75	5.13

**Figure 6.** Root mean square error (RMSE) of the validated models based on the red-edge normalized difference vegetation index (NDVI_{red-edge}).

(Fava et al., 2007; Gao et al., 2000; Mutanga and Skidmore, 2004). Better performances of NDVI_{red-edge} and CI_{red-edge} stem from the fact that even though the red-edge part of the spectrum is characterized by lower absorption by chlorophyll, it still remains sensitive to changes in its content, reducing the saturation effect and enhancing the sensitivity of these VIs to moderate–high vegetation densities (Clevers and Gitelson, 2013; Wu et al., 2008).

Incorporating PAR_m into the model resulted in a general decrease in the goodness of fit of the linear regression. One reason for this is that sunlight is used by plants more efficiently under cloudy than clear sky conditions due to a more uniform illumination of the canopy, and thus a smaller fraction of the canopy likely to be light saturated (Baldocchi and Amthor, 2001; Chen et al., 2009; Mercado et al., 2009). Accordingly, significantly higher photosynthesis rates under diffuse as regards direct radiation conditions (with similar values of PAR) were noted in the Monte Bondone site (Fig. 5). Similar results have been reported by Rossini et al. (2012), who also pointed out that, in a similar subalpine grassland ecosystem, the inclusion of incident PAR in a model formulation did not result in an improved estimation

of GEP. However, in several other studies referring to other dynamic ecosystems, GEP was successfully estimated as a product of VIs and PAR (Peng and Gitelson, 2012; Rossini et al., 2010; Wu et al., 2009). A recent study of Peng et al. (2013) confirmed that the use of PAR in the model can introduce noise and unpredictable uncertainties in GEP estimations. As suggested by these authors, the response of productivity to changes in PAR is quite complex and is influenced by many variables such as vegetation physiological status, canopy structure and light distribution in the canopy. Some other authors also brought to light some important aspects related to the use of PAR. Sims et al. (2008) showed that the variation in PAR is a more relevant determinant of GEP over very short timescales, and appears to be important for diurnal trends. Gitelson et al. (2012) demonstrated that seasonal variation of PAR potential (defined as the maximal value of incident PAR that may occur when the concentrations of atmospheric gasses and aerosols are minimal) can be used to improve the performance of the models. Therefore, further analyses of the response of different vegetation types to various levels of diffuse radiation are required, and the hypothesis that the DI and PAR potential can improve the performance of the models including radiation as an input parameter needs to be verified.

The use of the reflectance approach instead of the VI approach did not lead to considerably improved results in estimating GEP_m. Including additional predictors in multiple stepwise regression resulted in only a 6 % improvement of the explained variance, considering all of the 5 years of observations collectively. We believe this was partly due to the limited number of available bands of the CROPSCAN system, and that further studies are needed to explore the benefits of using hyperspectral data for predicting CO₂ uptake across different terrestrial ecosystem types.

A detailed analysis of the full vegetation spectrum and of the various spectral absorption features appears to be particularly meaningful for providing a solid basis for upscaling of GEP estimations using airborne and satellite platforms.

In this study the reflectance value at 720 nm, which was used in the multiple regression models, did not bring a relevant increase in the $\text{adj}R^2$ values (partial $\text{adj}R^2$ was 0.04 and

0.03 for model 3 and 4, respectively). On the other hand, the successful performance of VIs using this band confirms the important role of this part of the spectrum in monitoring the dynamics of ecosystem carbon dioxide fluxes.

Validation results of general model 1 fed with NDVI_{red-edge} showed that RMSE increased on average from 3.41 to 3.48 $\mu\text{mol m}^{-2} \text{s}^{-1}$, compared to non-validated general model 1 (averaging the values obtained from the 5 different validation years). Validation results of general model 4 showed that RMSE increased on average from 3.06 to 3.26 $\mu\text{mol m}^{-2} \text{s}^{-1}$, compared to non-validated general model 4. The highest decrease of the GEP_m estimation accuracy was noted in the growing season of 2012 (Table 4, Fig. 6), which was presumably caused by the unusual drought which occurred just after the cut event. The precipitation to temperature ratio for a 15-day period after the cut in the growing season of 2012 was more than 10 times lower than in the other years, and this fact could have affected GEP_m to a higher extent than VIs related to canopy “greenness”. As a consequence, models calibrated with the first 4 years of the data set overestimated the GEP_m measured in the second part of the growing season of 2012.

During the observation period, the study site experienced a high variability in both precipitation and air temperature (covering approximately 88 % and 54 % of the variability observed in a 20-year period for precipitation and temperature, respectively) (Fig. 2). General model 1 parameterized with NDVI_{red-edge} ($\text{adj}R^2 = 0.74$), and general model 3 ($\text{adj}R^2 = 0.73$) and 4 ($\text{adj}R^2 = 0.79$) based on the reflectance data were successful in capturing the inter-annual variability of GEP_m among the 5 years characterized by different climatic conditions. Therefore, these results support the use of ground spectral measurements for monitoring GEP_m in a long-term framework. We must however emphasize that the possible limitation of the approach based on VIs related to “canopy greenness” is that variations of GEP due to the short term environmental stresses cannot be monitored by these VIs, unless these stresses affect chlorophyll content (Gitelson et al., 2008).

Combining proximal sensing with EC observations may be relevant also for the EC data gap filling. In fact, the accuracy and reliability of the EC measurements depend on certain theoretical assumptions (e.g., requirement for turbulent and non-advective atmospheric conditions, stationarity of the measured fluxes) which often cannot be fulfilled in real field conditions (Foken et al., 2004; Göckede et al., 2004; Papale et al., 2006). The need for rejecting data acquired during periods when the abovementioned micrometeorological conditions were not met or due to other reasons such as non-optimal wind directions, equipment failures etc. results in data set gaps constituting from 20 % to 60 % of annual data (Falge et al., 2001; Hui et al., 2004; Moffat et al., 2007). One of the most widely used gap-filling routines is based on the modeling of flux data with available environmental variables by means of nonlinear regression (Aubinet et al., 2000; Falge

et al. 2001). This technique uses two equations – one for the response of ecosystem respiration (R_{eco}) to temperature and one for the light response of GEP (Moffat et al., 2007) – allowing their predictions during gaps. The implementation of VIs into the light response model might help to improve the gap-filling results, especially in very dynamic ecosystems such as croplands, grasslands or deciduous forests. This could be particularly useful in case of long gaps in the EC data, which are inherently associated with a large degree of uncertainty (Moffat et al., 2007; Richardson and Hollinger, 2007; Wohlfahrt et al., 2010) and in case of managed ecosystems, where carbon dioxide uptake depends not only on the incoming radiation seasonality but also on cutting and grazing events. The results of a simple gap-filling approach presented in this study (based on creating and superimposing randomly distributed artificial gaps of three different lengths on the real data set and comparing GEP_m values derived from EC with GEP_m values filled with the best performing spectral models) encourage the use of spectral data in the gap-filling procedures of EC flux time series. The spectral based models were able to predict GEP_m values with a performance comparable with others methods (Moffat et al., 2007) with $\text{adj}R^2$ ranging from 0.70 (5-day-long gap, general model 1 parameterized with NDVI_{red-edge}) to 0.78 (1-day-long gap, general model 4 based on reflectance at 681, 720 and 781 nm and PAR_m data) (Table 6).

5 Conclusions

This study investigated the potential of a commercially available system – based on a 16-band multispectral sensor – for monitoring mean midday gross ecosystem production (GEP_m) in a dynamic subalpine grassland ecosystem of the Italian Alps. Chlorophyll-related indices including the red-edge part of the spectrum in their formulation (such as NDVI_{red-edge} and CI_{red-edge}) were the best predictors of GEP_m, and were able to explain most of its variability ($\text{adj}R^2 = 0.74$ for NDVI_{red-edge}, $\text{adj}R^2 = 0.73$ for CI_{red-edge}) during the 5 consecutive years of observations, characterized by different climatic conditions. Our results confirm the findings of the literature regarding the complexity of the response of ecosystem productivity to change in PAR (Peng et al., 2013). This response is influenced by many variables. In fact, in our study, the accuracy of GEP_m estimation decreased after including incident PAR_m into the linear regression model, and the photosynthesis process was shown to be more efficient under diffuse compared to direct radiation. Further investigations are planned in order to explore the utility of including DI and PAR potential in the models to improve their performances. Also, the use of the reflectance approach instead of the VI approach did not lead to considerably improved results in estimating GEP_m. Although a more detailed analysis of the full vegetation spectrum is desirable (for providing best performing algorithms and a solid basis for in situ

validation and upscaling of optical models to the airborne and satellite platforms), the results indicate that such relatively low-cost multispectral sensors can be adopted to provide a significant contribution in monitoring carbon dioxide fluxes and biophysical parameters in dynamic ecosystems, for improving gap-filling techniques and for further integration into more complex biogeochemical models.

Appendix A

Table A1. Spectral vegetation indices investigated in this study. R refers to reflectance at a specific band (nm).

Index	Formulation	Reference
NDVI	$(R750 - R681)/(R750 + R681)$ $(R781 - R681)/(R781 + R681)$ $(R861 - R681)/(R861 + R681)$	Rouse et al. (1973)
NDVI _{green}	$(R750 - R547)/(R750 + R547)$ $(R781 - R547)/(R781 + R547)$ $(R861 - R547)/(R861 + R547)$	Gitelson et al. (1996)
SR	R750/R681 R781/R681 R861/R681	Jordan (1969)
SR _{green}	R750/R547 R781/R547 R861/R547	Gitelson and Merzlyak (1997)
SR _{blue}	R470/R750 R470/R781 R470/R861	Zarco-Tejada et al. (2001)
MSR	$(R750/R681 - 1)/(R750/R681 + 1)^{1/2}$ $(R781/R681 - 1)/(R781/R681 + 1)^{1/2}$ $(R861/R681 - 1)/(R861/R681 + 1)^{1/2}$	Haboudane et al. (2004)
RDVI	$(R750 - R681)/(R750 + R681)^{1/2}$ $(R781 - R681)/(R781 + R681)^{1/2}$ $(R861 - R681)/(R861 + R681)^{1/2}$	Haboudane et al. (2004)
NDVI _{red-edge}	$(R750 - R720)/(R750 + R720)$ $(R781 - R720)/(R781 + R720)$ $(R861 - R720)/(R861 + R720)$	Gitelson and Merzlyak (1994)
MTCI	$(R750 - R720)/(R720 - R681)$ $(R781 - R720)/(R720 - R681)$ $(R861 - R720)/(R720 - R681)$	Dash and Curran (2004)
EVI	$2.5 \cdot (R750 - R681)/(1 + R750 + 6 \cdot R681 - 7.5 \cdot R470)$ $2.5 \cdot (R781 - R681)/(1 + R781 + 6 \cdot R681 - 7.5 \cdot R470)$ $2.5 \cdot (R861 - R681)/(1 + R861 + 6 \cdot R681 - 7.5 \cdot R470)$	Huete et al. (2002)
CI _{red-edge}	$(R750/R720) - 1$ $(R781/R720) - 1$ $(R861/R720) - 1$	Gitelson et al. (2003a)
CI _{green}	$(R750/R720) - 1$ $(R781/R720) - 1$ $(R861/R720) - 1$	Gitelson et al. (2003c)
Index	Formulation	Reference
PRI	$(R547 - R531)/(R547 + R531)$ $(R570 - R531)/(R570 + R531)$ $(R610 - R531)/(R610 + R531)$ $(R640 - R531)/(R640 + R531)$ $(R681 - R531)/(R681 + R531)$	Gamon et al. (1992)
mSR	$(R750 - R470)/(R720 - R470)$ $(R781 - R470)/(R720 - R470)$ $(R861 - R470)/(R720 - R470)$	Sims and Gamon (2002)
DR	$(R750 - R720)/(R750 - R681)$ $(R781 - R720)/(R781 - R681)$ $(R861 - R720)/(R861 - R681)$	Datt (1999)
mND	$(R750 - R720)/(R750 + R720 - 2R470)$ $(R781 - R720)/(R781 + R720 - 2R470)$ $(R861 - R720)/(R861 + R720 - 2R470)$	Sims and Gamon (2002)
mNDVI	$(R750 - R681)/(R750 + R681 - 2R470)$ $(R781 - R681)/(R781 + R681 - 2R470)$ $(R861 - R681)/(R861 + R681 - 2R470)$	Main et al. (2011)
VOG	R730/R720	Zarco-Tejada et al. (2001)
SIPI	$(R750 - R470)/(R750 - R681)$ $(R781 - R470)/(R781 - R681)$ $(R861 - R470)/(R861 - R681)$	Peñuelas et al. (1995)
SIPI 2	$(R750 - R547)/(R750 - R681)$ $(R781 - R547)/(R781 - R681)$ $(R861 - R547)/(R861 - R681)$	Blackburn (1998)
MCARI	$[(R720 - R681) - 0.2 \cdot (R720 - R547)]/(R720/R681)$	Daughtry et al. (2000)
MCARI 2	$[(R750 - R720) - 0.2 \cdot (R750 - R547)]/(R750/R720)$ $[(R781 - R720) - 0.2 \cdot (R781 - R547)]/(R781/R720)$ $[(R861 - R720) - 0.2 \cdot (R861 - R547)]/(R861/R720)$	Wu et al. (2008)
WDRVI	$(0.1 \cdot R750 - R681)/(0.1 \cdot R750 + R681)$ $(0.1 \cdot R781 - R681)/(0.1 \cdot R781 + R681)$ $(0.1 \cdot R861 - R681)/(0.1 \cdot R861 + R681)$	Gitelson (2004)
ISI	$(R781 - R750)$ $(R861 - R750)$	Vescovo et al. (2012)
NIDI	$(R781 - R750)/(R781 + R750)$ $(R861 - R750)/(R861 + R750)$	Vescovo et al. (2012)
WBI	R979/R902	Peñuelas et al. (1994)

Appendix B

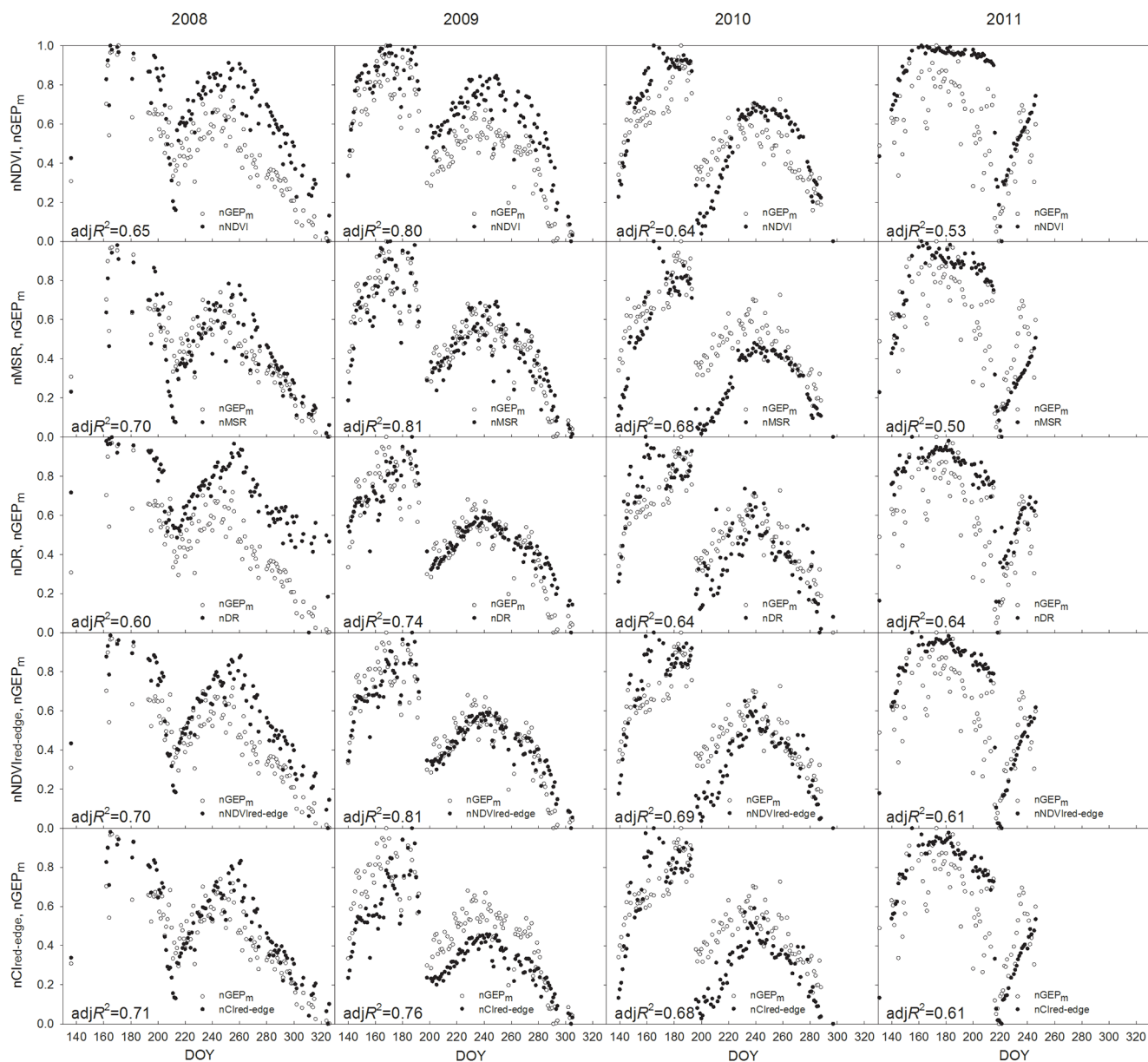


Figure B1. Seasonal courses of normalized spectral vegetation indices – nVIs (–) and normalized mean midday gross ecosystem production – nGEP_m (–) in the growing seasons of 2008–2011 (columns from left to right); adjR² between GEP_m estimated from EC measurements and GEP_m obtained with model 1 fed with the various VIs.

Acknowledgements. The authors would like to acknowledge Maurizio Bagnara, PhD student of Fondazione Edmund Mach, for help in R programming and John Gamon, Professor from University of Alberta, for fruitful discussions. The authors would like to thank the editor and the two reviewers (Anatoly Gitelson and the anonymous reviewer) of this manuscript for their valuable comments which have helped to improve the overall quality of the paper.

Edited by: G. Wohlfahrt

References

- Akaike, H.: Information theory and an extension of the maximum likelihood principle, in: *Proceedings of the Second International Symposium on Information Theory*, edited by: Petrov, B. N. and Csaki, F., Akademiai Kiado, Budapest, 267–281 (reproduced in: *Breakthroughs in Statistics*, edited by: Kotz, S. and Johnson, N. L., 2003), Vol. I, Foundations and Basic Theory, Springer-Verlag, New York, 610–624, 1973.
- Aubinet, M., Grelle, A., Ibrom, A., Rannik, Ü., Moncrieff, J., Foken, T., Kowalski, A. S., Martin, P. H., Berbigier, P., Bernhofer, C., Clement, R., Elbers, J., Granier, A., Grünwald, T., Morgenstern, K., Pilegaard, K., Rebmann, C., Snijders, W., Valentini, R., and Vesala, T.: Estimates of the annual net carbon and water exchange of forests: the EUROFLUX methodology, *Adv. Ecol. Res.*, 30, 113–175, 2000.
- Baldocchi, D. D.: Assessing the eddy covariance technique for evaluating carbon dioxide exchange rates of ecosystems: past, present and future, *Glob. Chang. Biol.*, 9, 479–492, 2003.
- Baldocchi, D. D. and Amthor, J. S.: Canopy photosynthesis: history, measurements, and models, in: *Terrestrial Global Productivity: Past, Present and Future*, edited by: Roy, J., Saugier, B., and Mooney, H., Academic Press, San Diego, 9–31, 2001.
- Balzarolo, M., Anderson, K., Nichol, C., Rossini, M., Vescovo, L., Arriga, N., Wohlfahrt, G., Calvet, J.-C., Carrara, A., Cerasoli, S., Cogliati, S., Daumard, F., Eklundh, L., Elbers, J. A., Evrendilek, F., Handcock, R. N., Kaduk, J., Klumpp, K., Longdoz, B., Matteucci, G., Meroni, M., Montagnani, L., Ourcival, J.-M., Sánchez-Cañete, E. P., Pontailler, J.-Y., Juszczak, R., Scholes, B., and Martín, M. P.: Ground-based optical measurements at European flux sites: a review of methods, instruments and current controversies, *Sensors*, 11, 7954–7981, doi:10.3390/s110807954, 2011.
- Blackburn, G. A.: Spectral indices for estimating photosynthetic pigment concentrations: a test using senescent tree leaves, *Int. J. Remote Sens.*, 19, 657–675, doi:10.1080/014311698215919, 1998.
- Burba, G.: *Eddy Covariance Method for Scientific, Industrial, Agricultural, and Regulatory Applications: a Field Book on Measuring Ecosystem Gas Exchange and Areal Emission Rates*, LICOR Biosciences, Lincoln, NE, USA, 2013.
- Canadell, J. G., Mooney, H. A., Baldocchi, D. D., Berry, J. A., Ehleringer, J. R., Field, C. B., Gower, S. T., Hollinger, D. Y., Hunt, J. E., Jackson, R. B., Running, S. W., Shaver, G. R., Steffen, W., Trumbore, S. E., Valentini, R., and Bond, B. Y.: Commentary: Carbon metabolism of the terrestrial biosphere: a multi-technique approach for improved understanding, *Ecosystems*, 3, 115–130, doi:10.1007/s100210000014, 2000.
- Carlson, T. N. and Ripley, D. A.: On the relation between NDVI, Fractional Vegetation Cover, and Leaf Area Index, *Remote Sens. Environ.*, 62, 241–252, 1997.
- Chen, J., Shen, M., and Kato, T.: Diurnal and seasonal variations in light-use efficiency in an alpine meadow ecosystem: causes and implications for remote sensing, *J. Plant Ecol.*, 2, 173–185, doi:10.1093/jpe/rtp020, 2009.
- Clevers, J. G. P. W. and Gitelson, A. A.: Remote estimation of crop and grass chlorophyll and nitrogen content using red-edge bands on Sentinel-2 and -3, *Int. J. Appl. Earth Obs.*, 23, 344–351, doi:10.1016/j.jag.2012.10.008, 2013.
- Dash, J. and Curran, P. J.: The MERIS terrestrial chlorophyll index, *Int. J. Remote Sens.*, 25, 5403–5413, doi:10.1080/0143116042000274015, 2004.
- Datt, B.: A new reflectance index for remote sensing of chlorophyll content in higher plants: tests using eucalyptus leaves, *J. Plant Physiol.*, 154, 30–36, doi:10.1016/S0176-1617(99)80314-9, 1999.
- Daughtry, C. S. T., Walthall, C. L., Kim, M. S., Brown de Colstoun, E., and McMurtrey III, J. E.: Estimating corn leaf chlorophyll concentration from leaf and canopy reflectance, *Remote Sens. Environ.*, 74, 229–239, 2000.
- Falge, E., Baldocchi, D., Olson, R., Anthoni, P., Aubinet, M., Bernhofer, C., Burba, G., Ceulemans, R., Clement, R., Dolman, H., Granier, A., Gross, P., Grünwald, T., Hollinger, D., Jensen, N.-O., Katul, G., Keronen, P., Kowalski, A., Lai, C. T., Law, B. E., Meyers, T., Moncrieff, J., Moors, E., Munger, J. W., Pilegaard, K., Rannik, Ü., Rebmann, C., Suyker, A., Tenhunen, J., Tu, K., Verma, S., Vesala, T., Wilson, K., and Wofsy, S.: Gap filling strategies for defensible annual sums of net ecosystem exchange, *Agr. Forest Meteorol.*, 107, 43–69, doi:10.1016/S0168-1923(00)00225-2, 2001.
- Fava, F., Parolo, G., Colombo, R., Gusmeroli, F., Della Marianna, G., Monteiro, A. T., and Bocchi, S.: Fine-scale assessment of hay meadow productivity and plant diversity in the European Alps using field spectrometric data, *Agr. Ecosyst. Environ.*, 137, 151–157, 2010.
- Foken, T., Göckede, M., Mauder, M., Mahrt, L., Amiro, B., and Munger, W.: Post-field data quality control, in: *Handbook of Micrometeorology*, 181–208, 2004.
- Gamon, J. A., Peñuelas, J., and Field, C. B.: A narrow-waveband spectral index that track diurnal changes in photosynthetic efficiency, *Remote Sens. Environ.*, 41, 35–44, 1992.
- Gamon, J. A., Rahman, A. F., Dungan, J. L., Schildhauer, M., and Huemmrich, K. F.: Spectral Network (SpecNet) – what is it and why do we need it?, *Remote Sens. Environ.*, 103, 227–235, doi:10.1016/j.rse.2006.04.003, 2006.
- Gamon, J. A., Coburn, C., Flanagan, L., Huemmrich, K. F., Kidde, C., Sanchez-Azofeifa, G. A., Thayer, D., Vescovo, L., Gianelle, D., Sims, D., Rahman, A. F., and Zonta Pastorella, G.: SpecNet revisited: bridging flux and remote sensing communities, *Can. J. Remote Sens.*, 36, 376–390, doi:10.5589/m10-06, 2010.
- Gao, X., Huete, A. R., Ni, W., and Miura, T.: Optical–biophysical relationships of vegetation spectra without background contamination, *Remote Sens. Environ.*, 74, 609–620, 2000.
- Geider, R. J., Delucia, E. H., Falkowski, P. G., Finzi, A. C., Grime, J. P., Grace, J., Kana, T. M., Roche, J. L. A., Long, S. P., Osborne, B. A., Platt, T., Prentice, I. C., Raven, J. A.,

- Schlesinger, W. H., Smetacek, V., Stuart, V., Sathyendranath, S., Thomas, R. B., Vogelmann, T. C., Williams, P., and Woodward, I. F.: Primary productivity of planet earth: biological determinants and physical constraints in terrestrial and aquatic habitats, *Glob. Chang. Biol.*, 7, 849–882, 2001.
- Gianelle, D. and Vescovo, L.: Determination of green herbage ratio in grasslands using spectral reflectance – methods and ground measurements, *Int. J. Remote Sens.*, 28, 931–942, doi:10.1080/01431160500196398, 2007.
- Gianelle, D., Vescovo, L., Marcolla, B., Manca, G., and Cescatti, A.: Ecosystem carbon fluxes and canopy spectral reflectance of a mountain meadow, *Int. J. Remote Sens.*, 30, 435–449, doi:10.1080/01431160802314855, 2009.
- Gitelson, A. A.: Wide Dynamic Range Vegetation Index for remote quantification of biophysical characteristics of vegetation, *J. Plant Physiol.*, 161, 165–73, doi:10.1078/0176-1617-01176, 2004.
- Gitelson, A. and Merzlyak, M. N.: Quantitative experiments estimation of chlorophyll-a using reflectance spectra: experiments with autumn chestnut and maple leaves, *J. Photochem. Photobiol.*, 22, 247–252, 1994.
- Gitelson, A. A. and Merzlyak, M. N.: Remote estimation of chlorophyll content in higher plant leaves, *Int. J. Remote Sens.*, 18, 2691–2697, 1997.
- Gitelson, A. A., Kaufman, Y. J., and Merzlyak, M. N.: Use of a green channel in remote sensing of global vegetation from EOS-MODIS, *Remote Sens. Environ.*, 58, 289–298, 1996.
- Gitelson, A. A., Gritz, Y., and Merzlyak, M. N.: Relationships between leaf chlorophyll content and spectral reflectance and algorithms for non-destructive chlorophyll assessment in higher plant leaves, *J. Plant Physiol.*, 160, 271–282, doi:10.1078/0176-1617-00887, 2003a.
- Gitelson, A. A., Verma, S. B., Viña, A., Rundquist, D. C., Keydan, G., Leavitt, B., Arkebauer, T. J., Burba, G. G., and Suyker, A. E.: Novel technique for remote estimation of CO₂ flux in maize, *Geophys. Res. Lett.*, 30, 1486, doi:10.1029/2002GL016543, 2003b.
- Gitelson, A. A., Viña, A., Arkebauer, T. J., Rundquist, D. C., Keydan, G., and Leavitt, B.: Remote estimation of leaf area index and green leaf biomass in maize canopies, *Geophys. Res. Lett.*, 30, 1148, doi:10.1029/2002GL016450, 2003c.
- Gitelson, A. A., Viña, A., Ciganda, V., Rundquist, D. C., and Arkebauer, T. J.: Remote estimation of canopy chlorophyll content in crops, *Geophys. Res. Lett.*, 32, L08403, doi:10.1029/2005GL022688, 2005.
- Gitelson, A. A., Viña, A., Verma, S. B., Rundquist, D. C., Arkebauer, T. J., Keydan, G., Leavitt, B., Ciganda, V., Burba, G. G., and Suyker, A. E.: Relationship between gross primary production and chlorophyll content in crops: implications for the synoptic monitoring of vegetation productivity, *J. Geophys. Res.*, 111, D08S11, doi:10.1029/2005JD006017, 2006.
- Gitelson, A. A., Viña, A., Masek, J. G., Verma, S. B., and Suyker, A. E.: Synoptic Monitoring of Gross Primary Productivity of Maize Using Landsat Data, *IEEE Geosci. Remote Sens. Lett.*, 5, 133–137, 2008.
- Gitelson, A. A., Peng, Y., Masek, J. G., Rundquist, D. C., Verma, S., Suyker, A., Baker, J. M., Hatfield, J. L., and Meyers, T.: Remote estimation of crop gross primary production with Landsat data, *Remote Sens. Environ.*, 121, 404–414, doi:10.1016/j.rse.2012.02.017, 2012.
- Glenn, E. P., Huete, A. R., Nagler, P. L., and Nelson, S. G.: Relationship between remotely-sensed vegetation indices, canopy attributes, and plant physiological processes: what vegetation indices can and cannot tell us about the landscape, *Sensors*, 8, 2136–2160, 2008.
- Göckede, M., Rebmann, C., and Foken, T.: A combination of quality assessment tools for eddy covariance measurements with footprint modelling for the characterisation of complex sites, *Agr. Forest Meteorol.*, 127, 175–188, doi:10.1016/j.agrformet.2004.07.012, 2004.
- Haboudane, D., Miller, J. R., Pattey, E., Zarco-Tejada, P. J., and Strachan, I. B.: Hyperspectral vegetation indices and novel algorithms for predicting green LAI of crop canopies: modeling and validation in the context of precision agriculture, *Remote Sens. Environ.*, 90, 337–352, doi:10.1016/j.rse.2003.12.013, 2004.
- Harris, A. and Dash, J.: The potential of the MERIS Terrestrial Chlorophyll Index for carbon flux estimation, *Remote Sens. Environ.*, 114, 1856–1862, doi:10.1016/j.rse.2010.03.010, 2010.
- Huete, A., Didan, K., Miura, T., Rodriguez, E. P., Gao, X., and Ferreira, L. G.: Overview of the radiometric and biophysical performance of the MODIS vegetation indices, *Remote Sens. Environ.*, 83, 195–213, doi:10.1016/S0034-4257(02)00096-2, 2002.
- Hui, D., Wan, S., Su, B., Katul, G., Monson, R., and Luo, Y.: Gap-filling missing data in eddy covariance measurements using multiple imputation (MI) for annual estimations, *Agr. Forest Meteorol.*, 121, 93–111, doi:10.1016/S0168-1923(03)00158-8, 2004.
- Inoue, Y., Peñuelas, J., Miyata, A., and Mano, M.: Normalized difference spectral indices for estimating photosynthetic efficiency and capacity at a canopy scale derived from hyperspectral and CO₂ flux measurements in rice, *Remote Sens. Environ.*, 112, 156–172, doi:10.1016/j.rse.2007.04.011, 2008.
- Jackson, R. D. and Huete, A. R.: Interpreting vegetation indices, *Prev. Vet. Med.*, 11, 185–200, 1991.
- Jordan, C. F.: Derivation of leaf area index from quality of light on the forest floor, *Ecology*, 50, 663–666, 1969.
- Kljun, N., Rotach, M. W., and Schmid, H. P.: A three-dimensional backward lagrangian footprint model for a wide range of boundary-layer stratifications, *Bound.-Lay. Meteorol.*, 103, 205–226, 2001.
- Lobell, D. B., Asner, G. P., Ortiz-Monasterio, J. I., and Benning, T. L.: Remote sensing of regional crop production in the Yaqui Valley, Mexico: estimates and uncertainties, *Agr. Ecosyst. Environ.*, 1944, 1–16, 2002.
- Main, R., Cho, M. A., Mathieu, R., O’Kennedy, M. M., Ramoelo, A., and Koch, S.: An investigation into robust spectral indices for leaf chlorophyll estimation, *ISPRS J. Photogramm.*, 66, 751–761, doi:10.1016/j.isprs.2011.08.001, 2011.
- Marcolla, B. and Cescatti, A.: Experimental analysis of flux footprint for varying stability conditions in an alpine meadow, *Agr. Forest Meteorol.*, 135, 291–301, doi:10.1016/j.agrformet.2005.12.007, 2005.
- Marcolla, B., Cescatti, A., Manca, G., Zorer, R., Cavagna, M., Fiora, A., Gianelle, D., Rodeghiero, M., Sottocornola, M., and Zampedri, R.: Climatic controls and ecosystem responses drive the inter-annual variability of the net ecosystem exchange of an alpine meadow, *Agr. Forest Meteorol.*, 151, 1233–1243, doi:10.1016/j.agrformet.2011.04.015, 2011.

- Mason, R. L., Gunst, R. F., and Hess, J. L.: Variable selection techniques, in: *Statistical Design and Analysis of Experiments with Applications to Engineering and Science*, John Wiley & Sons, Hoboken, New Jersey, 672–674, 2003.
- Mercado, L. M., Bellouin, N., Sitch, S., Boucher, O., Huntingford, C., Wild, M., and Cox, P. M.: Impact of changes in diffuse radiation on the global land carbon sink, *Nature*, 458, 1014–1017, doi:10.1038/nature07949, 2009.
- Moffat, A. M., Papale, D., Reichstein, M., Hollinger, D. Y., Richardson, A. D., Barr, A. G., Beckstein, C., Braswell, B. H., Churkina, G., Desai, A. R., Falge, E., Gove, J. H., Heimann, M., Hui, D., Jarvis, A. J., Kattge, J., Noormets, A., and Stauch, V. J.: Comprehensive comparison of gap-filling techniques for eddy covariance net carbon fluxes, *Agr. Forest Meteorol.*, 147, 209–232, doi:10.1016/j.agrformet.2007.08.011, 2007.
- Moncrieff, J. B., Massheder, J. M., de Bruin, H., Elbers, J., Friborg, T., Heusinkveld, B., Kabat, P., Scott, S., Soegaard, H., and Verhoef, A.: A system to measure surface fluxes of momentum, sensible heat, water vapour and carbon dioxide, *J. Hydrol.*, 188–189, 589–611, doi:10.1016/S0022-1694(96)03194-0, 1997.
- Monteith, J. L.: Solar radiation and productivity in tropical ecosystems, *J. Appl. Ecol.*, 9, 747–766, 1972.
- Monteith, J. L. and Moss, C. J.: Climate and the efficiency of crop production in Britain, *Philos. T. R. Soc. B*, 281, 277–294, doi:10.1098/rstb.1977.0140, 1977.
- Mutanga, O. and Skidmore, A.: Narrow band vegetation indices overcome the saturation problem in biomass estimation, *Int. J. Remote Sens.*, 25, 3999–4014, 2004.
- Myneni, R. B. and Williams, D. L.: On the relationship between FAPAR and NDVI, *Remote Sens. Environ.*, 49, 200–211, 1994.
- O'Brien, R. M.: A caution regarding rules of thumb for variance inflation factors, *Qual. Quant.*, 41, 673–690, doi:10.1007/s11135-006-9018-6, 2007.
- Papale, D., Reichstein, M., Aubinet, M., Canfora, E., Bernhofer, C., Kutsch, W., Longdoz, B., Rambal, S., Valentini, R., Vesala, T., and Yakir, D.: Towards a standardized processing of Net Ecosystem Exchange measured with eddy covariance technique: algorithms and uncertainty estimation, *Biogeosciences*, 3, 571–583, doi:10.5194/bg-3-571-2006, 2006.
- Peng, Y. and Gitelson, A. A.: Remote estimation of gross primary productivity in soybean and maize based on total crop chlorophyll content, *Remote Sens. Environ.*, 117, 440–448, doi:10.1016/j.rse.2011.10.021, 2012.
- Peng, Y., Gitelson, A. A., Keydan, G., Rundquist, D. C., and Moses, W.: Remote estimation of gross primary production in maize and support for a new paradigm based on total crop chlorophyll content, *Remote Sens. Environ.*, 115, 978–989, doi:10.1016/j.rse.2010.12.001, 2011.
- Peng, Y., Gitelson, A. A., and Sakamoto, T.: Remote estimation of gross primary productivity in crops using MODIS 250 m data, *Remote Sens. Environ.*, 128, 186–196, 2013.
- Peñuelas, J., Gamon, J. A., Fredeen, A. L., Merino, J., and Field, C. B.: Reflectance indices associated with physiological changes in nitrogen and water-limited sunflower leaves, *Remote Sens. Environ.*, 48, 135–146, 1994.
- Peñuelas, J., Baret, F., and Filella, I.: Semi-empirical indices to assess carotenoids/chlorophyll a ratio from leaf spectral reflectance, *Photosynthetica*, 31, 221–230, 1995.
- Richardson, A. D. and Hollinger, D. Y.: A method to estimate the additional uncertainty in gap-filled NEE resulting from long gaps in the CO₂ flux record, *Agr. Forest Meteorol.*, 147, 199–208, doi:10.1016/j.agrformet.2007.06.004, 2007.
- Rossini, M., Meroni, M., Migliavacca, M., Manca, G., Cogliati, S., Busetto, L., Picchi, V., Cescatti, A., Seufert, G., and Colombo, R.: High resolution field spectroscopy measurements for estimating gross ecosystem production in a rice field, *Agr. Forest Meteorol.*, 150, 1283–1296, doi:10.1016/j.agrformet.2010.05.011, 2010.
- Rossini, M., Cogliati, S., Meroni, M., Migliavacca, M., Galvagno, M., Busetto, L., Cremonese, E., Julitta, T., Siniscalco, C., Morra di Cella, U., and Colombo, R.: Remote sensing-based estimation of gross primary production in a subalpine grassland, *Biogeosciences*, 9, 2565–2584, doi:10.5194/bg-9-2565-2012, 2012.
- Rouse, J. W., Haas, R. H., Schell, J. A., and Deering, D. W.: Monitoring vegetation systems in the Great Plains with ERTS, in: *Third ERTS Symposium, NASA SP-353*, vol. 1, US Government Printing Office, Washington DC, 309–317, 1973.
- Running, S. W., Baldocchi, D. D., Turner, D. P., Gower, S. T., Bakwin, P. S., and Hibbard, K. A.: A global terrestrial monitoring network integrating tower fluxes, flask sampling, ecosystem modeling and EOS satellite data, *Remote Sens. Environ.*, 70, 108–127, 1999.
- Schmid, H. P.: Source areas for scalars and scalar fluxes, *Bound.-Lay. Meteorol.*, 67, 293–318, doi:10.1007/BF00713146, 1994.
- Serrano, L., Filella, I., and Peñuelas, J.: Remote sensing of biomass and yield of winter wheat under different nitrogen supplies, *Crop Sci.*, 40, 723–731, 2000.
- Sims, D. A. and Gamon, J. A.: Relationships between leaf pigment content and spectral reflectance across a wide range of species, leaf structures and developmental stages, *Remote Sens. Environ.*, 81, 337–354, doi:10.1016/S0034-4257(02)00010-X, 2002.
- Sims, D. A., Luo, H., Hastings, S., Oechel, W. C., Rahman, A. F., and Gamon, J. A.: Parallel adjustments in vegetation greenness and ecosystem CO₂ exchange in response to drought in a Southern California chaparral ecosystem, *Remote Sens. Environ.*, 103, 289–303, doi:10.1016/j.rse.2005.01.020, 2006.
- Sims, D., Rahman, a, Cordova, V., Elmasri, B., Baldocchi, D., Bolstad, P., Flanagan, L., Goldstein, a, Hollinger, D., and Misson, L.: A new model of gross primary productivity for North American ecosystems based solely on the enhanced vegetation index and land surface temperature from MODIS, *Remote Sens. Environ.*, 112, 1633–1646, doi:10.1016/j.rse.2007.08.004, 2008.
- Sjöström, M., Ardö, J., Eklundh, L., El-Tahir, B. A., El-Khidir, H. A. M., Hellström, M., Pilesjö, P., and Seaquist, J.: Evaluation of satellite based indices for gross primary production estimates in a sparse savanna in the Sudan, *Biogeosciences*, 6, 129–138, doi:10.5194/bg-6-129-2009, 2009.
- Stenberg, P., Rautiainen, M., Manninen, T., Voipio, P., and Smolander, H.: Reduced Simple Ratio Better than NDVI for Estimating LAI in Finnish Pine and Spruce Stands, *Silva Fenn.*, 38, 3–14, 2004.
- Vescovo, L. and Gianelle, D.: Mapping the green herbage ratio of grasslands using both aerial and satellite-derived spectral reflectance, *Agr. Ecosyst. Environ.*, 115, 141–149, doi:10.1016/j.agee.2005.12.018, 2006.

- Vescovo, L. and Gianelle, D.: Using the MIR bands in vegetation indices for the estimation of grassland biophysical parameters from satellite remote sensing in the Alps region of Trentino (Italy), *Adv. Space Res.*, 41, 1764–1772, doi:10.1016/j.asr.2007.07.043, 2008.
- Vescovo, L., Wohlfahrt, G., Balzarolo, M., Pilloni, S., Sottocornola, M., Rodeghiero, M., and Gianelle, D.: New spectral vegetation indices based on the near-infrared shoulder wavelengths for remote detection of grassland phytomass, *Int. J. Remote Sens.*, 33, 2178–2195, 2012.
- Viña, A., Gitelson, A. A., Nguy-Robertson, A. L., and Peng, Y.: Comparison of different vegetation indices for the remote assessment of green leaf area index of crops, *Remote Sens. Environ.*, 115, 3468–3478, doi:10.1016/j.rse.2011.08.010, 2011.
- Walter-Shea, E. A., Privette, J., Cornell, D., Mesarch, M. A., and Hays, C. J.: Relations between directional spectral vegetation indices and leaf area and absorbed radiation in Alfalfa, *Remote Sens. Environ.*, 61, 162–177, 1997.
- Wohlfahrt, G., Pilloni, S., Hörtnagl, L., and Hammerle, A.: Estimating carbon dioxide fluxes from temperate mountain grasslands using broad-band vegetation indices, *Biogeosciences*, 7, 683–694, doi:10.5194/bg-7-683-2010, 2010.
- Wu, C., Niu, Z., Tang, Q., and Huang, W.: Estimating chlorophyll content from hyperspectral vegetation indices: modeling and validation, *Agr. Forest Meteorol.*, 148, 1230–1241, doi:10.1016/j.agrformet.2008.03.005, 2008.
- Wu, C., Niu, Z., Tang, Q., Huang, W., Rivard, B., and Feng, J.: Remote estimation of gross primary production in wheat using chlorophyll-related vegetation indices, *Agr. Forest Meteorol.*, 149, 1015–1021, doi:10.1016/j.agrformet.2008.12.007, 2009.
- Xiao, X., Zhang, Q., Braswell, B., Urbanski, S., Boles, S., Wofsy, S., Moore III, B., and Ojima, D.: Modeling gross primary production of temperate deciduous broadleaf forest using satellite images and climate data, *Remote Sens. Environ.*, 91, 256–270, doi:10.1016/j.rse.2004.03.010, 2004.
- Zarco-Tejada, P. J., Miller, J. R., Noland, T. L., Mohammed, G. H., and Sampson, P. H.: Scaling-up and model inversion methods with narrowband optical indices for chlorophyll content estimation in closed forest canopies with hyperspectral data, *IEEE T. Geosci. Remote*, 39, 1491–1507, doi:10.1109/36.934080, 2001.